Polym. Bull. (2011) 67:1293–1309
DOI 10.1007/s00289-011-0494-z

ORIGINAL PAPER

Gas barrier and morphology characteristics of linear low-density polyethylene and two different polypropylene films

Mia Kurek · Damir Klepac · Mario Ščetar · Kata Galić · Srećko Valić · Yong Liu · Weimin Yang

Received: 20 January 2011 / Accepted: 20 April 2011 / Published online: 5 May 2011

Abstract In this research, linear low-density polyethylene (PE-LLD), cast polypropylene (PPcast), and bioriented coextruded polypropylene (BOPP) were used as polymeric materials. Permeability, diffusivity, and solubility of N_2, O_2, and CO_2 through above polymers were obtained at different temperatures. The structure and thermal–mechanical features of the films were characterized by scanning electron microscopy (SEM) and differential scanning calorimetry (DSC). The permeability, diffusivity, solubility, and their temperature dependency were studied by correlations

M. Kurek · M. Ščetar · K. Galić (✉)
Faculty of Food Technology and Biotechnology, University of Zagreb, Pierottijeva 6, HR-10000 Zagreb, Croatia
e-mail: kgalic@pbf.hr

M. Kurek
e-mail: mkurek@pbf.hr

M. Ščetar
e-mail: mscetar@pbf.hr

D. Klepac · S. Valić
School of Medicine, University of Rijeka, Braće Branchetta 20, HR-51000 Rijeka, Croatia
e-mail: dklepac@medri.hr

S. Valić
e-mail: valics@medri.hr

S. Valić
Rudjer Bošković Institute, Bijenička c. 54, HR-10000 Zagreb, Croatia

Y. Liu · W. Yang
College of Mechanical and Electrical Engineering, Beijing University of Chemical Technology, No. 15, Beisanhuan East Road, Beijing 100029, China
e-mail: yongsd@iccas.ac.cn

W. Yang
e-mail: yangwm@mail.buct.edu.cn

with gas molecule properties. The highest permeation coefficients (>3.8 × 10^{-8} cm^3 cm^{-1} s^{-1} bar^{-1}) are obtained for PPcast at 60 °C. Activation energy for permeation follows the sequence: $N_2 > O_2 > CO_2$ for PE-LLD and PPcast. On the other hand, the diffusion activation energy follows the order: $O_2 > CO_2 > N_2$ and $N_2 > CO_2 > O_2$ for PE-LLD and PPcast, respectively. In the case of BOPP, activation energy follows the sequence: $O_2 > CO_2 > N_2$; $CO_2 > N_2 > O_2$; and $O_2 > CO_2 > N_2$ for permeation, diffusion, and heat of sorption, respectively.

Keywords Activation energy · Polyolefins · Differential scanning calorimetry (DSC) · Gas permeation

Introduction

With the increase of application and demand of polymer materials in packaging market and with the fast development of new functional materials, the development and testing of barrier films is not only limited to parameters such as permeability coefficient and transmission rate, it is more frequently to test the diffusion and solution coefficient that affect permeation parameters directly. Polyethylene (PE) and polypropylene (PP) are two of the most widely used polymers in the food and beverage packaging industry. PP offers high resistance to water vapor permeation and is widely used in rigid as well as flexible food packaging applications. PP films can be oriented, which improves their barrier properties, mechanical strength, and optical properties. These properties can be varied over a wide range by the choice of the manufacturing process. Linear low-density polyethylene films (PE-LLD) show great commercial potential in the packaging industry due to their well-known good mechanical properties, specifically good processibility, increased stiffness in molded parts, and high resistance to tearing and toughness [1].

The study of polymer crystallization kinetics is important from theoretical and practical points of view, and many researchers have studied the crystallization behavior of different polyethylenes [2–6].

The selection of a barrier polymer for a particular packaging application depends not only on its barrier properties but also on other physical properties and a comparison of physical, mechanical, and optical properties as well.

Oxygen is a critical mass transfer component in a number of deteriorative reactions that can have an effect on the shelf-life of many packaged foods. The permeability of gases such as oxygen, nitrogen, and carbon dioxide through polymeric materials increases as temperature increases but the extent of these changes varies for different polymers [7]. Knowledge of the quality kinetics associated with specific food products has permitted development of mathematical models to predict shelf-life from data collected at elevated storage temperatures [8].

Villaluenga et al. [9] showed that the permeability and its temperature dependence do not show a noticeable influence on the processing conditions. The effect of processing conditions on the diffusivity seems to be more complex. Differences were observed for different PE-LLD films in the diffusion coefficients,

in the case of oxygen, and in their change with the temperature, which was particularly marked in the case of carbon dioxide [9].

Holden et al. [10] thorough study on the effect of orientation on the gas permeability of PE-LLD showed a large reduction of diffusion coefficient with increasing draw ratio. Campaň et al. [11] observed that diffusion measurements provide a sensitive method of detecting structural changes, particularly in the non-crystalline region. Studies on the temperature dependence of both the permeability and mechanical properties of coextruded PE-LLD films suggest that melting and crystallization processes occurring above room temperature presumably affect the permeability and diffusion coefficients of gases through them [11].

Barrier properties are usually highly temperature dependent which can greatly influence the shelf-life of packaged food. Thus, the purpose of this article is to describe the change with the temperature of the apparent coefficients of permeability, diffusion, and solubility of oxygen, nitrogen, and carbon dioxide in PE-LLD and two different PP films.

Materials and methods

Investigated test films are listed and specified in Table 1. Films are obtained, without graphics, directly from producer, Aluflexpack d.o.o., Umag, Croatia.

Permeability measurement

Gas permeance (q/cm^3 m^{-2} day^{-1} bar^{-1}) determination is performed using manometric method, on permeability testing appliance, Type GDP-C [12]. The increase in pressure during the test period is evaluated and displayed by an external computer. Using the Method A, suitable for monofilms, it is possible to obtain permeability (P/cm^3 cm^{-1} s^{-1} bar^{-1}), solubility (S/cm^3 cm^{-3} bar^{-1}), and diffusion (D/cm^2 s^{-1}) coefficients. The coefficient values as well as the time lag (τ_L) value are calculated from known sample thickness. Data are recorded and evaluated by a PC. The PC is connected to the GDP-C with a serial interface.

The sample temperature, within the range of 4 and 60 °C, is adjusted using an external Thermostat (HAAKE F3 with Waterbath K).

The temperature dependence of permeability and diffusivity are modeled using Arrhenius equations of the following forms:

Table 1 Polymers used in the experiments

Polymer	Abbreviation	Thickness/μm
Linear low-density polyethylene	PE-LLD	50
Cast polypropylene	PPcast	30
Biaxially oriented coextruded polypropylene	BOPP	20

Activation Energy for Permeation:

$$P = P_o \exp(-E_p/RT) \quad (1)$$

Activation Energy for Diffusion:

$$D = D_o \exp(-E_d/RT) \quad (2)$$

Heat of Sorption:

$$S = S_o \exp(-H_s/RT) \quad (3)$$

where P_o, D_o, and S_o are pre-exponential factors, E_p and E_d are activation energies for permeation and diffusion, respectively, in J mol^{-1}, H_s is heat of sorption in J mol^{-1}, R is gas constant in J mol^{-1} K^{-1}, and T is temperature in K

A permselectivity, P_A/P_B, separated to diffusivity selectivity, D_A/D_B, and solubility selectivity, S_A/S_B, for gas A to gas B, is described as follows:

$$\frac{P_A}{P_B} = \left(\frac{D_A}{D_B}\right) \cdot \left(\frac{S_A}{S_B}\right) \quad (4)$$

DSC

The degrees of crystallinity (χ_c) of samples were determined by measuring the heat of fusion of the samples by differential scanning calorimetry (DSC) analysis and dividing these values by the heats of fusion for 100% crystalline polymers, taken from the literature [13]. DSC measurements were performed at a heating rate of 10 °C/min in a nitrogen atmosphere on a Mettler-Toledo DSC822e differential scanning calorimeter calibrated by indium. Thermograms were recorded using 10 mg of samples in the temperature range from 25 to 150 °C for PE and from 25 to 200 °C for cast polypropylene (PPcast) and bioriented coextruded polypropylene (BOPP). The heats of fusion for the 100% crystalline PE and PPs were taken to be 293 and 190 J/g, respectively, according to Brandrup [13].

SEM and EDS measurements

The microstructure of polymeric samples was observed using Hitachi S-4700 scanning electron microscopy (SEM, Hitachi S4700, 20 kV accelerating voltage, Japan). Element constitutes of a small area were analyzed using an INCA Energy Dispersive X-ray Spectrometer (EDS) (Netherlands) joined to S-4700 SEM. The samples were sprayed with platinum for 5 min before being observed.

Statistical analyses

Analysis of variance (ANOVA), at a significance level of $\alpha = 0.05$, was applied to analyzed parameters. All statistical procedures were performed using STATISTICA, version 7 (StatSoft, Inc., USA).

For each of the above parameters (q, P, D, S), three complete series of experiments were conducted (in triplicate). The averages of the observed values for the three experiments, at a given conditions, were obtained and used in the subsequent analyses.

Results and discussion

DSC thermograms of PE-LLD and PPs samples are presented in Fig. 1. All investigated samples show first-order endothermic peak which corresponds to the melting of crystalline phase. Contrary to PPcast and BOPP, the first-order peak of PE-LLD shows two types of endothermic contributions: the main peak at 109 °C and "shoulder" peak at 122 °C. This seems to be an intrinsic property of the crystalline structure of used PE-LLD sample, since this picture remains unchanged after multiple runs. Such an effect might be a consequence of crystal reorganization caused by the temperature increase. More precisely, the multiplicity of an endothermic peak in polymers is usually explained as a solid phase transition from one crystallographic modification to another occurring when $T < T_m$ [14]. The results obtained by DSC analysis, summarized in Table 2, are in good agreement with previous measurements [7]. An increase in the degree of crystallinity and melting temperature has been observed in BOPP film compared to PPcast film. The increase in the degree of crystallinity can be related to the effect of strain-induced crystallization, while the shift of melting temperature to higher value could be the result of a decrease in the amorphous phase entropy [15].

The impact of temperature, polymer, and gas on barrier characteristics is presented in Table 3. Unlike gas type ($p > 0.05$), temperature and polymer type significantly impacted permeance, permeability (P), diffusivity (D), and solubility (S) coefficients ($p < 0.05$).

The crystallinity (Fig. 2) was determined on the samples that were previously subject to temperature-dependent permeability measurements.

Analyzed polymers differ in the amount of crystallinity as indicated in Table 2 and Fig. 2. PE-LLD shows higher crystallinity changes with temperature increase.

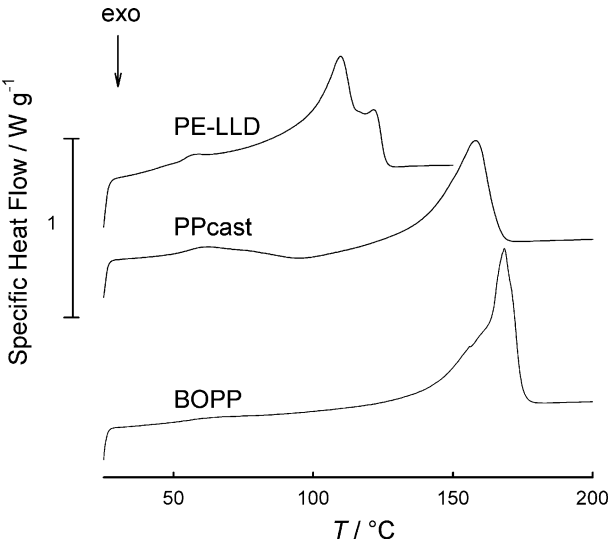

Fig. 1 DSC thermograms of polymeric films

Table 2 Melting point (T_m), heat of fusion (ΔH_f), and degree of crystallinity (χ_c) for as received polymeric films, measured by DSC

Sample	T_m/°C	ΔH_f/J g^{-1}	χ_c/%
PE-LLD	109	90	31
PPcast	158	82	43
BOPP	168	89	47

Table 3 ANOVA univariate tests of significance for analyzed polymers

Effects	p ($\alpha = 0.05$)			
	q, cm^3 m^{-2} day^{-1} bar^{-1}	P, cm^3 cm^{-1} s^{-1} bar^{-1}	D, cm^2 s^{-1}	S, cm^3 cm^{-3} bar^{-1}
Intercept	0.000000	0.000000	0.000000	0.000000
Temperature	0.000000	0.000000	0.000173	0.000001
Polymers	0.000270	0.000011	0.000000	0.000000
Gas	0.940467	0.922187	0.276646	0.523514

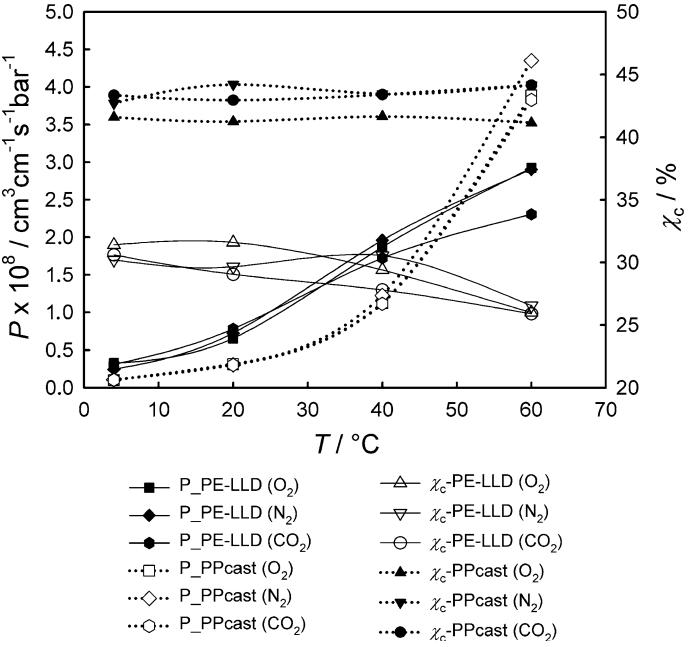

Fig. 2 Permeability (P) and crystallinity values (χ_c) for PE-LLD and PPcast samples at different temperatures

The lowest crystallinity (26%) is recorded for PE-LLD film exposed to permeability measurement at 60 °C. Identical behavior of PE (75 μm) film after tempering at 60 °C was found by Mrkić et al. [7].

Permeation through polymer films occurs almost exclusively in the noncrystalline region. This accounts for the relationship between permeation rates and crystalline content—the higher the crystalline content, the lower the permeability. This works better in the case of PE-LLD than PPcast. A film's crystalline alignment/orientation can alter its permeability by affecting the pathways available for diffusion. Various papers have considered this principle, often referring to it as a tortuosity factor [15, 16]. Permeability would be lower in films having a crystalline orientation that creates a more tortuous pathway. Sophisticated analytical methods, such as small angle or wide angle X-ray scattering (SAXS or WAXS), birefringence, Raman spectroscopy, and various high-resolution microscopic techniques have been used to characterize the crystalline structure of polymers. Numerous studies have utilized these analytical methods to define the crystalline structure of PE [17–19] and some have attempted to correlate crystalline structure and permeation properties [17, 18]. However, these test methods are not commonly available and most studies have yet to successfully correlate permeability and crystalline structure properties using these methods.

Breaks in the Arrhenius plots (Figs. 3, 4) in all samples can be observed. The break temperature is found at 20 and 40 °C. This effect is less evident in the diffusion (Fig. 3) than in the solubility (Fig. 4) curves and less significant in CO_2 and N_2 than in O_2 (especially in the case of PE-LLD). According to literature data [11, 20, 21], the breaks observed in PE films may be caused by α relaxation process, produced by motions of the chain folds at the crystal surface.

Among the analyzed polymers, PE-LLD shows the highest diffusion (Fig. 3) and the lowest solubility (Fig. 4) coefficients for all gases. Contrary to literature data [21, 22], P and D values of CO_2 are lower than that of oxygen, due to higher solubility (Fig. 4).

Generally, lower permeability (data not presented) properties of BOPP film, among the investigated samples, is mainly due to kinetic effects, i.e., very low

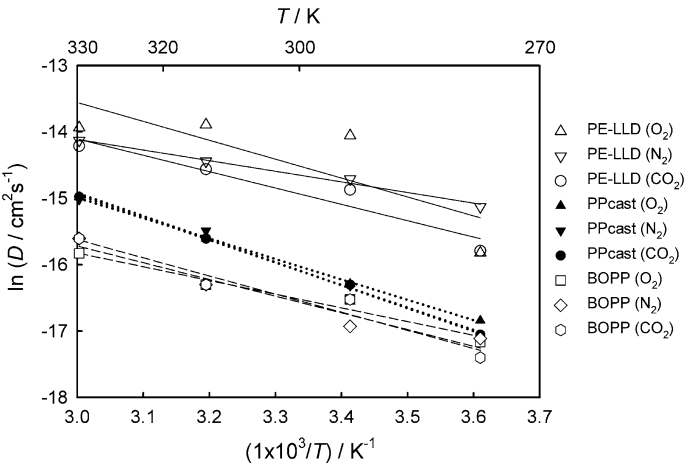

Fig. 3 Arrhenius plots for the diffusion coefficient of gases for PE-LLD and PPs films

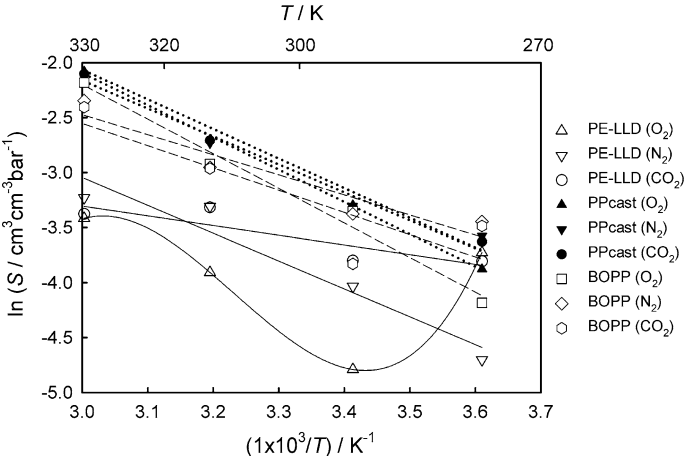

Fig. 4 Arrhenius plots for the solubility coefficient of gases for PE-LLD and PPs films

diffusion coefficients (Fig. 3). It was previously found that the decrease in oxygen permeability of biaxially drawn PP films was due primarily to a decrease in the diffusivity [23–25]. According to the free volume concepts of gas transport, diffusivity derives from the dynamic-free volume. These concepts readily account for the general observations that gas permeability is reduced by increasing the crystallinity and by increasing the amorphous phase density [26, 27]. However, for the stretched films, the decrease in permeability was accompanied by decreasing density, which combined lower crystallinity (more amorphous phase) and lower amorphous phase density (higher free volume) [28]. Positron annihilation lifetime spectroscopy (PALS) measurements on similar films showed that the stretching conditions did not affect the free volume hole size [29]. The result appeared to be inconsistent with conventional free volume concepts of gas permeability. Biaxial orientation reduced the oxygen permeability of the oriented films, however, the reduction did not correlate with the amount of orientation (measured by birefringence), with the fraction of amorphous phase (determined by density) or with the free volume hole size (determined by PALS). Rather, the decrease in permeability was attributed to reduced mobility of amorphous tie molecules [29].

Gas solubility (Fig. 4) in polymers, similar to permeability (Fig. 2), increases with temperature increase. These changes, also observed by Villaluenga et al. [9] for PE-LLD films, might be due to the melting of small and less perfect crystalline entities. This melting process might increase the solubility of the gases in the films and favor the ease of the gas diffusion due to the decrease of the obstruction of the diffusion paths. Slight decrease in CO_2 and N_2 solubility (Fig. 4) coefficient in PE-LLD occurred at 40 and 60 °C. This was also observed by Laguna et al. [30]. At the higher temperature range (40–60 °C), crystallinity decreased from 6 to 13% for the PE-LLD samples (Fig. 2). In the case of PPcast, crystallinity decrease was only 1.2% after O_2 permeability. After N_2 and CO_2 permeability measurements, crystallinity increased in the range of 1.6 and 1.7%, respectively.

Excellent correlation between polymer crystallinity and permeability coefficients (P, D, and S) is obtained (from −0.52 to −0.998). Positive correlation was observed for PPcast samples for N_2 (0.516–0.554) and CO_2 (0.871–0.929) only.

According to the literature [31], the time lag (τ_L), which is a measure of the time delay between the start and the point at which the diffusion process reaches a steady state, there are some models in which the smaller gas particles permeate faster. In fact, the size, shape, and concentration of free volume holes available in a polymer control the rate of gas diffusion and its permeation [32]. Higher D values mean that the τ_L (Fig. 5) for the gas flowing through the films decreases. This effect was especially evident for oxygen diffusion (Fig. 3) in the temperature range from 4 to 20 °C. A high correlation values are obtained between τ_L and gas diffusivity, from −0.91 to −0.99, from −0.84 to −0.88, and from −0.85 to −0.93 for PE-LLD, PPcast, and BOPP, respectively.

The presence of crystalline regions complicates the process, and the most pronounced effect is a reduction in diffusivity. In fact, crystals make a type of mechanical barrier, and therefore, regardless the lower density of amorphous phase, the diffusion is slower in the presence of crystalline phase.

SEM analyses (Fig. 6a, b) showed some defects on the surface of the treated samples. Relative distribution of the defects in the matrix of olefins can have a significant impact on both the diffusivity and solubility coefficient of the penetrant. Presence of the fillers has been also detected. From the element content (EDS data), the filler is identified as SiO_2 (Fig. 6c). According to manufacture, a small quantity of antiblocking silica is incorporated into a film formulation in order to avoid handling problems. Osman et al. [33] reported that the incorporation of fillers in PE-LLD increases the elastic modulus of the material and can increase its tensile strength also, but it almost invariably decreases the elongation at break.

Filler particles can influence the molecular absorption behavior in two principal ways. Where the solubility of the filler differs from the polymer matrix then the absorption can be either increased or decreased depending on the relative solubility of the molecule in the matrix and filler. Most common inorganic filler particles (e.g., glass or carbon fibers, talc, clays, silica) can usually be considered as impermeable in comparison to polymer matrix. The presence of filler particles can also affect the

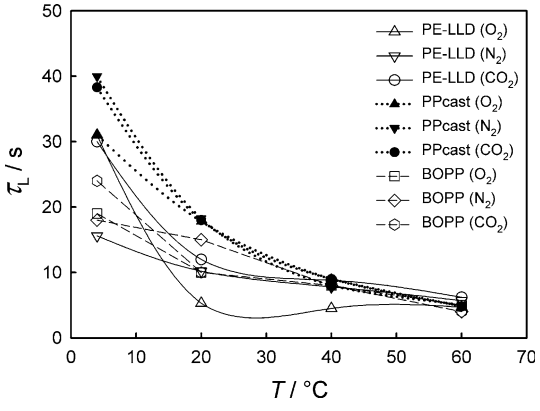

Fig. 5 Changes of the time lag values with the temperature increase for PE-LLD and PPs samples

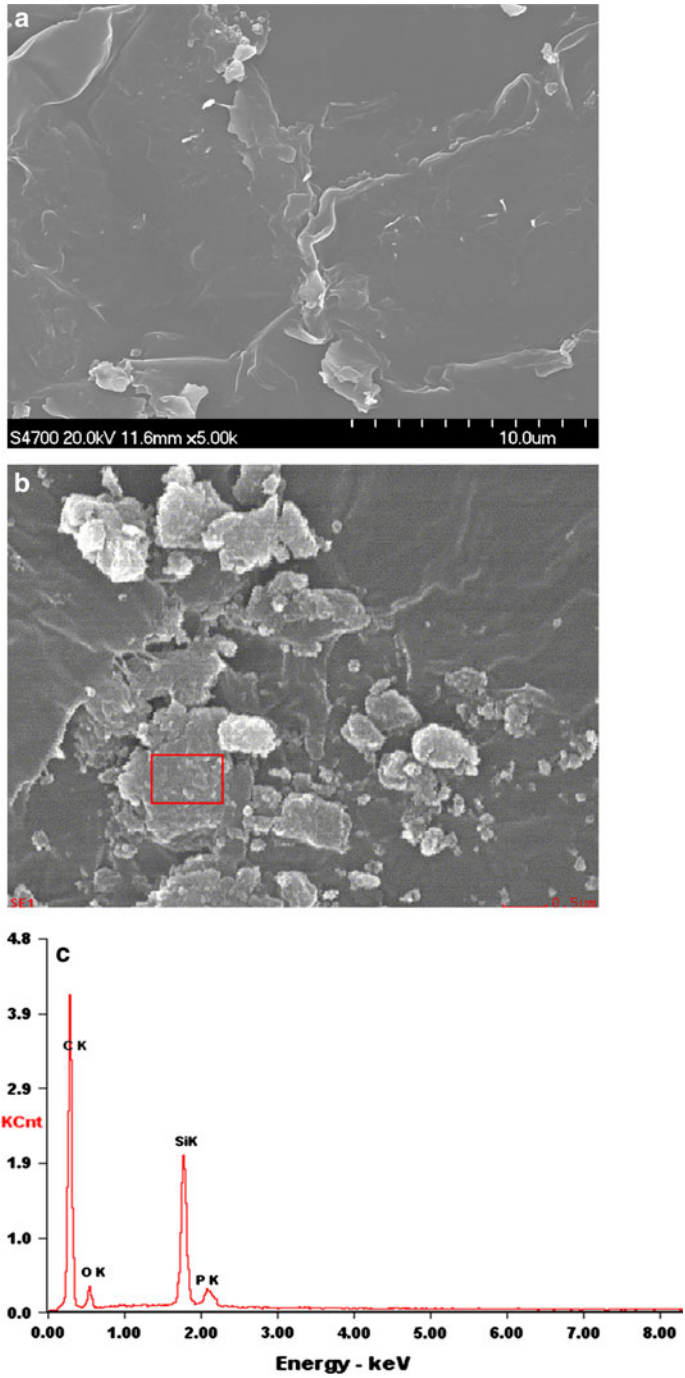

Fig. 6 SEM analyses of the **a** PE-LLD and **b** PPcast samples after nitrogen permeability measurement at 60 °C, **c** EDS data for PPcast sample

diffusion behavior. Diffusing molecules would need to work their way around impermeable particles, increasing path lengths and reducing mass transport rates. Improved barrier properties from nano-sized fillers would be expected from the increased lengths of diffusion paths [34].

It seems that this was not the case of the investigated samples as diffusivity (Fig. 3) increases (with an exception of oxygen in PE-LLD above 40 °C). This is probably due to not well-dispersed filler in the polymer matrix as well as minor microvoids presence. Furthermore, crystallinity (Fig. 2) of PE-LLD continuously decreases (15% average).

The activation energy (Table 4) for gas permeation is significantly higher than the activation energy for the gas diffusion for analyzed polymers. This suggests that gas diffusion through film may not be a single-activated process as a consequence of the morphological changes caused by recrystallization process. These results imply on the differences both in the structure of polymer matrix and the impact of the temperature and the properties of the penetrant, respectively.

Similar values in activation energies of permeation, in undrawn and both longitudinal and transverse drawing of PE-LLD films in the low-temperature interval (25–55 °C) was found by Villaluenga and Seoane [35].

Virtually nothing is known today regarding a possibility to correlate activation energies of diffusion and gas permeation in polymers. These properties can be of interest per se as physicochemical characteristics of energy barriers in mass transfer of small molecules through a polymeric matrix. Practical importance of these parameters stems from the fact that they are needed for calculations of gas diffusion and permeation rates at elevated and low temperatures. It is always much easier to relate the transport parameters, and activation energies in particular, with the properties of gases (Table 5) than those of polymers. For a given polymer, activation energies of permeation and diffusion increase proportionally with the second power of collision diameter of gas molecules [36, 37].

Since polymer films possess both solid and liquid properties, an effective molecule diameter for gases (the square root of the product of gas collision diameter and kinetic diameter), which describes the relationship between diffusivity and gas molecule diameter, is correlated with activation energy for gas permeability and diffusivity. PPcast and BOPP show an excellent correlation between effective molecule diameter (Table 4) and the activation energy for gas diffusion (positive correlation), as well as heat of sorption (negative correlation). Opposite correlation is observed for PE-LLD.

Collision diameter is a widely accepted correlating parameter for diffusivities in relatively high mobility rubber or liquid media [40]. Positive correlation between collision diameter and $E_a(D)$ was found for PPcast and BOPP (Table 4).

It was reported that the solubility increases as Lennard-Jones force constant (indication of molecular interaction) or critical temperature (measure of the ease of condensation for gaseous molecules) increases [39, 41]. In fact, excellent correlation between Lenard-Jones constants with heat of sorption was obtained for PPcast film (Table 4). Correlation between Van der Waals constant a, which is a measure of the attraction force between the molecules, while the term b is due to the finite volume of the molecules and to their general incompressibility

Table 4 Correlation ($r \geq 0.5$) between the activation energy (kJ mol^{-1}) for gas permeation, $E_a(P)$, diffusion, $E_a(D)$, and heat of sorption (H_s) for analyzed polymers and gas properties

	$E_a(P)$			$E_a(D)$			H_s		
	PE-LLD	PPcast	BOPP	PE-LLD	PPcast	BOPP	PE-LLD	PPcast	BOPP
O_2	31	49.9	43.3	23.7	25.5	17.2	7.5	24.4	26.2
N_2	34	51.2	36.1	13.4	28.8	21	21.1	22.4	15.2
CO_2	27.8	49.4	39.5	20.5	28.2	22.7	7.3	21.1	16.8
Critical values									
V/cm^3 mol^{-1}	−0.25	0.02	−0.75	−0.56	0.92	1	0.27	−0.99	−0.93
T/K	−0.94	−0.81	0.12	0.36	0.2	0.63	−0.63	−0.7	−0.24
p/atm	−1	−0.94	0.39	0.61	−0.08	0.39	−0.83	−0.47	0.05
Van der Waals									
a/L^2 bar mol^{-2}	0.87	0.71	0.04	−0.21	−0.35	−0.74	0.5	0.8	0.39
b/L mol^{-1}	−0.39	−0.14	−0.64	−0.43	0.85	1	0.13	−1	−0.87
$C_{p,m}$/J K^{-1} mol^{-1} $= a + bT + c/T^2$									
a	−0.91	−0.77	0.04	0.29	0.27	0.68	−0.58	−0.75	−0.3
b/10^{-3} K^{-1}	−0.91	−0.76	0.04	0.28	0.27	0.69	−0.57	−0.75	−0.31
c/10^5 K^2	0.93	0.8	−0.1	−0.34	−0.22	−0.64	0.62	0.71	0.25
$\Delta_{trs}H^{\theta}$/kJ mol^{-1}									
T_f/K	−0.85	−0.68	−0.08	0.17	0.39	0.77	−0.47	−0.83	−0.42
Fusion	−0.86	−0.69	−0.06	0.18	0.37	0.76	−0.48	−0.82	−0.41
T_b/K	−0.92	−0.78	0.068	0.31	0.25	0.67	−0.59	−0.73	−0.28
Vaporization	−0.9	−0.75	0.02	0.27	0.29	0.71	−0.56	−0.76	−0.33
298 K									
M/g mol^{-1}	−0.96	−0.86	0.21	0.44	0.11	0.56	−0.7	−0.63	−0.15
S_m^{θ}/J K^{-1} mol^{-1}	0.79	0.61	0.18	−0.07	−0.48	−0.83	0.38	0.88	0.51
Lennard-Jones									
(ε/k)/K	−0.95	−0.83	0.15	0.39	0.17	0.6	−0.66	−0.67	−0.2
r_o/pm	0.66	−0.44	−0.36	−0.12	0.63	0.92	−0.2	−0.95	−0.66
At 1 bar									
κ/J K^{-1} m^{-1} s^{-1} (273 K)	0.85	0.68	0.07	−0.17	−0.38	−0.77	0.47	0.82	0.42
η/mP (273 K)	0.52	0.28	0.52	0.29	−0.76	−0.94	0.02	0.99	0.78
Collision cross-section, σ/nm^2	−0.73	−0.53	−0.27	−0.03	0.56	0.88	−0.29	−0.92	−0.59
Kinetic diameter σ_k/cm 10^{-8}	1	0.98	−0.5	−0.7	0.2	−0.27	0.89	0.36	−0.17
Collision diameter σ_c/cm 10^{-8}	−0.57	−0.34	−0.47	−0.23	0.72	0.96	−0.08	−0.98	−0.75
Effective diameter σ_{eff}/cm 10^{-8}	0.11	0.37	−0.93	−0.82	1	0.91	0.59	−0.86	−1

[42], and heat of sorption, as well as $E_a(D)$, is obtained for PPcast and BOPP, respectively. PE-LLD shows excellent correlation between the kinetic diameter, which is close to the molecular sieving dimension of a gas and is a sensitive

Table 5 The most important properties of gases used in the experiments [38, 39]

Properties	Nitrogen	Carbon dioxide	Oxygen
Critical volume (cm^3 mol^{-1})	90.10	94	78
Critical temperature (K)	126.3	304.2	154.8
Critical pressure (atm)	33.54	72.85	50.14
Van der Waals constant, a/L^2 bar mol^{-2}	1.352	3.610	1.364
Van der Waals constant, b/L mol^{-1}	0.0387	0.0429	0.0319
Temperature variation of molar heat capacities $C_{p,m}$/J K^{-1} mol^{-1} $= a + bT + c/T^2$			
a	28.58	44.22	29.96
$b/10^{-3}$ K^{-1}	3.77	8.79	4.18
$c/10^5$ K^2	−0.50	−8.62	−1.67
Standard enthalpies of fusion and vaporization at the transition temperature, $\Delta_{trs}H^{\theta}$/kJ mol^{-1}			
T_f/K	63.15	217	54.36
Fusion	0.719	8.33	0.444
T_b/K	77.35	194.6	90.18
Vaporization	5.586	25.23 *s*	6.820
Thermodynamic data at 298 K			
M/g mol^{-1}	28.013	44.010	31.999
S_m^{θ}/J K^{-1} mol^{-1}	191.61	117.6	205.138
Lennard-Jones potential parameters			
(ε/k)/K	91.85	201.71	113.27
r_o/pm	391.9	444.4	365.4
Collision cross-section, σ/nm^2	0.43	0.52	0.40
Transport properties of gases at 1 bar			
κ/J K^{-1} m^{-1} s^{-1} (273 K)	0.0240	0.0145	0.0245
η/μP (273 K)	166	136	195
Kinetic diameter, σ_k/cm 10^{-8}	3.64	3.3	3.46
Collision diameter, σ_c/cm 10^{-8}	3.68	4.0	3.43
Effective diameter, σ_{eff}/cm 10^{-8}	3.66	3.63	3.44

s sublimation

measure of ability to move in highly restrictive environments [39], and $E_a(P)$, $E_a(D)$, and H_s values.

Unlike PE-LLD and PPcast films, BOPP generally shows good correlation between gas properties (Table 5) and $E_a(D)$ value (with exception of critical pressure and kinetic diameter) but not with $E_a(P)$ and H_s values (Table 4).

According to Dias et al. [29], no correlation was found between O_2 permeability and n_z, which is a measure of the orientation in the thickness direction, i.e., the direction of gas transport. It has been suggested that this unprecedented control of the molecular structure can lead to a set of differentiated properties of oriented film. The controlling factor was thought to be the reduced mobility of stretched tie chains that control the frequency with which connecting channels form between free volume holes [28]. The extent to which the tie chains were stretched and tightened

depended on the stress applied to the film. This resulted in a systematic decrease in permeability as the film experienced increasingly higher stresses during stretching.

The interactions between the gas molecules and the pore wall at the pore opening have been considered and integrated to determine a suction energy from which certain information about the gas kinetics can be obtained [43]. This novel approach provides a theoretical determination of the size of pores in which different modes of diffusion occur for each gas. Using a minimum pore size for Kundsen transport obtained with proposed model ($O_2 = 13.36$; $N_2 = 14.08$ and $CO_2 = 13.04$ Å), positive correlation with $E_a(P)$ is obtained for PE-LLD (0.97) and PPcast (1.00) and negative for BOPP (−0.65). The minimum pore sizes for barrier-free transport of each gas are in the same order as the kinetic diameter, with slightly different values because the model takes into account the interaction with the pore wall and not kinetic size only.

Because the food respiration process and film permeability are both temperature dependent, changes in respiration rate due to temperature changes should be balanced by changes in film permeability to maintain the desired steady-state gas composition. The results of Al-Ati and Hotchkiss [44] suggest that packaging films with CO_2/O_2 permselectivities lower than those commercially available (<3) would further optimize O_2 and CO_2 concentrations in MAP of respiring produce, particularly highly respiring and minimally processed produce.

Generally, the highest CO_2/O_2 permselectivity difference between the polymers analyzed is obtained at 20 °C (Fig. 7). Comparing gas permeability coefficients (P, D, and S) with CO_2/O_2 selectivity, only PPcast shows good correlation with diffusion (0.74) and solubility selectivity (−0.55). In the case of PE-LLD and BOPP, good correlation is obtained for permselectivity (−0.69) and diffusion selectivity (0.94), respectively.

Among the investigated monofilms, the highest O_2/CO_2 permselectivity (data not presented) is obtained for BOPP (1.61), which agrees well with data obtained by Mrkić et al. [45]. It was also reported that permselectivity of polyolefins is strongly influenced by flavor absorption [46] and stress applied [45].

In food packaging, barrier characteristics have become an important safety tool, thus further research on this issue is of great importance. Free volume has been

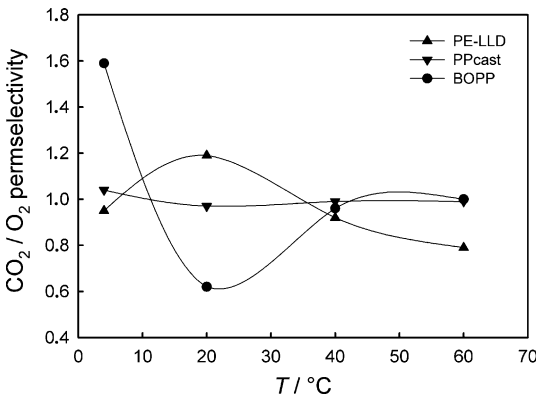

Fig. 7 CO_2/O_2 permselectivitiy changes with temperature

shown to have strong influence on gas diffusivity in polymers [16, 47]. There exist different formulations of free volume theory, but neither involves a concept of activation energy, although all of them attempt to relate free volume or a part of it with diffusion rate of a gas in the medium. This and similar observations will be further investigate and correlate with the $E_a(P)$, $E_a(D)$, and H_s values with free volume analysis of food packaging polymers.

Conclusions

Similar gas (N_2, CO_2, and O_2) permeance values for the PE-LLD (4.2×10^2 to 3.4×10^3 cm^3 m^{-2} day^{-1} bar^{-1}) and PPcast (2.9×10^2 to 3.5×10^3 cm^3 m^{-2} day^{-1} bar^{-1}) are obtained in the temperature range from 4 to 40 °C. The lowest permeance values are obtained for BOPP (2.3×10^2 to 1.9×10^3 cm^3 m^{-2} day^{-1} bar^{-1}) in the same temperature range. The lowest solubility of gases is obtained for PE-LLD. For example, the O_2 solubility in PE-LLD varies from 2.41×10^{-2} cm^3 cm^{-3} bar^{-1} for 31.4% crystallinity to 3.28×10^{-2} cm^3 cm^{-3} bar^{-1} for 26% crystallinity, at 4 and 60 °C, respectively.

The activation energy for gas permeation, ranged from 27.8 to 34.0 and from 49.4 to 51.2 kJ mol^{-1} for PE-LLD and PPcast, respectively, correlates well with the properties of the penetrants.

The activation energy for gas permeation is significantly higher than the activation energy for the gas diffusion. This suggests that gas diffusion through film may not be a single-activated process as a consequence of the morphological changes caused by recrystallization process.

Acknowledgments This paper is part of the activities within the Croatian-Chinese project. Authors gratefully acknowledge the support provided by the Ministry of Science, Education and Sports of the Republic of Croatia (MZOS), and Ministry of Science and Technology (China). Authors from Croatia thank the MZOS for financial support under projects: 062-0000000-3209 and 058-1252971-2805.

References

1. Robertson GL (2006) Food packaging principles and practice, 2nd edn. CRC Press, Boca Raton, FL
2. Hussein IA (2008) Nonisothermal crystallization kinetics of linear metallocene polyethylenes. J Appl Polym Sci 107:2802–2809. doi:10.1002/app.27392
3. Feng L, Kamal MR (2005) Spherulitic crystallization behavior of linear low-density polyethylene. Polym Eng Sci 45:74–83. doi:10.1002/pen.20231
4. Feng L, Kamal MR (2005) Crystallization and melting behavior of homogeneous and heterogeneous linear low-density polyethylene resins. Polym Eng Sci 45:1140–1151. doi:10.1002/pen.20389
5. Zhang M, Lynch DT, Wanke SE (2000) Characterization of commercial linear low-density polyethylene by TREF-DSC and TREF-SEC cross-fractionation. J Appl Polym Sci 75:960–967. doi:10.1002/(SICI)1097-4628(20000214)75:7<960:AID-APP13>3.0.CO;2-R
6. Zhang M, Lynch DT, Wanke SE (2001) Effect of molecular structure distribution on melting and crystallization behavior of 1-butene/ethylene copolymers. Polymer 42:3067–3075. doi:10.1016/S0032-3861(00)00667-4
7. Mrkić S, Galić K, Ivanković M, Hamin S, Ciković N (2006) Gas transport and thermal characterization of mono- and di-polyethylene films used for food packaging. J Appl Polym Sci 99:1590–1599. doi:10.1002/app.22513

8. de Blackburn CW (2000) Modelling shelf-life. In: Kilcast D, Subramaniam P (eds) The stability and shelf-life of food. CRC Press/Woodhead Publishing Limited, Cambridge
9. Villaluenga JPG, Seoane B, Compan V (1998) Diffusional characteristics of coextruded linear low-density polyethylenes prepared from different conditions of processing. J Appl Polym Sci 70:23–37. doi:10.1002/(SICI)1097-4628(19981003)70:1<23:AID-APP5>3.0.CO;2-W
10. Holden PS, Orchard GAJ, Ward IM (1985) A study of the gas barrier properties of highly oriented polyethylene. J Polym Sci Polym Phys 23:709–731. doi:10.1002/pol.1985.180230408
11. Compañ V, Diaz-Calleja R, Ribes A, Andrio A, López ML, Riande E (1996) Mechanical relaxations and diffusive changes in linear low density polyethylene (LLDPE) films subject to induced stretching. J Appl Polym Sci 60:767–778. doi:10.1002/(SICI)1097-4628(19960502)60:5<767:AID-APP16>3.0.CO;2-W
12. Brugger Feinmechanik GmbH (1993) Gas permeability testing manual. Registergericht Müchen HRB 77020
13. Brandrup J (1989) Polymer handbook, vol 109. Wiley, New York
14. Bershtein VA, Egorov VM (1994) Differential scanning calorimetry of polymers. Physics, chemistry, analysis, technology. Ellis Horwood, New York
15. Srinivas S, Brant P, Huang Y, Paul DR (2003) Structure and properties of oriented polyethylene films. Polym Eng Sci 43:831–849. doi:10.1002/pen.10069
16. Monge MA, Villaluenga JPG, Muñoz A, Leguey T, Pareja R (2002) Annealing-induced enhancement of the gas diffusivity in coextruded LLDPE films investigated by positron lifetime spectroscopy. Macromolecules 35:8088–8092. doi:10.1021/ma020484e
17. Vittoria V (1995) Influence of the crystallinity on the transport properties of polyethylene. J Mater Sci 30:3954–3958. doi:10.1007/BF01153962
18. Hedenqvist M, Angelstok A, Edsberg L, Larsson PT, Gedde UW (1996) Diffusion of small-molecule penetrants in polyethylene—free volume and morphology. Polymer 37:2887–2902. doi:10.1016/0032-3861(96)89384-0
19. Mathot VBF, Scherrenberg RL, Pijpers TFJ (1998) Metastability and order in linear, branched and copolymerized polyethylenes. Polymer 39:4541–4559. doi:10.1016/S0032-3861(97)10306-8
20. Compañ V, Andrio A, López ML, Alvarez C, Riande E (1997) Effect of time of annealing on gas permeation through coextruded linear low-density polyethylene (LLDPE) films. Macromolecules 30:3317–3322. doi:10.1021/ma960691c
21. Garcia-Villaluenga JP, Seoane B, Compañ V, Diaz-Calleja R (1997) Thermomechanical and diffusive studies in films prepared from copolymers of ethylene-1-octene subject to longitudinal and transversal induced stretching. Polymer 38:3827–3836. doi:10.1016/S0032-3861(96)00942-1
22. Compañ V, Ribes A, Diaz-Calleja R, Riande E (1996) Permeability of co-extruded linear low-density polyethylene films to oxygen and carbon dioxide as determined by electrochemical techniques. Polymer 37:2243–2250. doi:10.1016/0032-3861(96)85870-8
23. Wang LH, Porter RS (1984) On the CO_2 permeation of uniaxially drawn polymers. J Polym Sci Polym Phys Ed 22:1645–1653. doi:10.1002/pol.1984.180220908
24. Chu F, Kimura Y (1996) Structure and gas permeability of microporous films prepared by biaxial drawing of beta-form polypropylene. Polymer 37:573–579. doi:10.1016/0032-3861(96)83143-0
25. Somlai LS, Liu RYF, Landoll LM, Hiltner A, Baer E (2005) Effect of orientation on the free volume and oxygen transport of a polypropylene copolymer. J Polym Sci B 43:1230–1243. doi:10.1002/polb.20412
26. Dlubek G, Saarinen K, Fretwell HM (1998) The temperature dependence of the local free volume in polyethylene and polytetrafluoroethylene—a positron lifetime study. J Polym Sci B 36:1513–1528. doi:10.1002/(SICI)1099-0488(19980715)36:9<1513:AID-POLB9>3.0.CO;2-K
27. Mashelkar RA, Kulkarni MG (1983) Unified altered free volume state model for transport phenomena in polymeric media. Pure Appl Chem 55:737–754
28. Lin YJ, Dias P, Chen HY, Hiltner A, Baer E (2008) Relationship between biaxial orientation and oxygen permeability of polypropylene film. Polymer 49:2578–2586. doi:10.1016/j.polymer.2008.03.033
29. Dias P, Lin YJ, Hiltner A, Baer E, Chen HY, Chum SP (2008) Effect of chain architecture on biaxial orientation and oxygen permeability of polypropylene film. J Appl Polym Sci 107:1730–1736. doi:10.1002/app.27197
30. Laguna MF, Guzmaán J, Riande E (2001) Transport of carbon dioxide in linear low-density polyethylene determined by permeation measurements and NMR spectroscopy. Polymer 42:4321–4327. doi:10.1016/S0032-3861(00)00809-0

31. Rutherford SW (2001) Polymer permeability and time lag at high concentrations of sorbate. J Membr Sci 183:101–107. doi:10.1016/S0376-7388(00)00579-2
32. Sodaye HS, Pujari PK, Goswami A, Manohar SB (1997) Probing the microstructure of Nafion-117 using positron annihilation spectroscopy. J Polym Sci B 35:771–776. doi:10.1002/(SICI)1099-0488(19970415)35:5<771:AID-POLB5>3.0.CO;2-P
33. Osman MA, Rupp JEP, Suter UW (2005) Tensile properties of polyethylene-layered silicate nanocomposites. Polymer 46:1653–1660. doi:10.1016/j.polymer.2004.11.112
34. Duncan B, Urquhart J, Roberts S (2005) Review of measurement and modelling of permeation and diffusion in polymers. NPL Report DEPC MPR 012
35. Villaluenga JPG, Seoane B (1998) Influence of drawing on gas transport mechanism in LLDPE films. Polymer 39:3955–3965. doi:10.1016/S0032-3861(98)00005-6
36. Meares P (1954) The diffusion of gases through polyvinyl acetate. J Am Chem Soc 76:3415–3422. doi:10.1021/ja01642a015
37. Teplyakov V, Meares P (1990) Correlation aspects of the selective gas permeabilities of polymeric materials and membranes. Gas Sep Purif 4:66–74. doi:10.1016/0950-4214(90)80030-O
38. Atkins P, De Paula J (2006) Physical chemistry, 8th edn. Oxford University Press, Oxford
39. Shieh JJ, Chung TS (1999) Gas permeability, diffusivity, and solubility of poly(4-vinylpyridine) film. J Polym Sci B 37:2851–2861. doi:10.1002/(SICI)1099-0488(19991015)37:20<2851:AID-POLB5>3.3.CO;2-L
40. Stannett V (1968) Simple gases. In: Crank J, Park GS (eds) Diffusion in polymers. Academic Press, New York
41. Michaels AS, Bixler HJ (1961) Solubility of gases in polyethylene. J Polym Sci 50:393–412. doi:10.1002/pol.1961.1205015411
42. Hodgman CD, Weast RC, Selby SM (1971) Handbook of chemistry and physics, 42nd edn. Chemical Rubber Publishing, Cleveland, OH
43. Thornton AW, Hilder T, Hill AJ, Hill JM (2009) Predicting gas diffusion regime within pores of different size, shape and composition. J Membr Sci 336:101–108. doi:10.1016/j.memsci.2009.03.019
44. Al-Ati T, Hotchkiss JH (2003) The role of packaging film permselectivity in modified atmosphere packaging. J Agric Food Chem 51:4133–4138. doi:10.1021/jf034191b
45. Mrkić S, Galić K, Ivanković M (2007) Effect of temperature and mechanical stress on barrier properties of polymeric films used for food packaging. J Plast Film Sheet 23:239–256. doi:10.1177/8756087907086102
46. Togawa J, Kanno T, Horiuchi J, Kobayashi M (2001) Gas permeability modification of polyolefin films induced by D-limonene swelling. J Membr Sci 188:39–48. doi:10.1016/S0376-7388(01)00374-X
47. Alentiev AY, Yampolskii YP (2000) Free volume model and trade off relations of gas permeability and selectivity in glassy polymers. J Membr Sci 165:201–216. doi:10.1016/S0376-7388(99)00229-X